RP Current Trends in Engineering and Technology
Vol. 2, No. 1 (January – March 2023) pp. 32–40
e-ISSN: 2583-5491

RESEARCH PLATEAU PUBLISHERS

Cite this article: J. Singh, Stimulated Raman scattering in weakly polar narrow band gap magnetized semiconductors in the presence of hot carriers, *RP Cur. Tr. Eng. Tech.* **2** (2023) 32–40.

Original Research Article

Stimulated Raman scattering in weakly polar narrow band gap magnetized semiconductors in the presence of hot carriers

Jaivir Singh
Department of Physics, J.V.M.G.R.R. College, Charkhi Dadri - 127306, Haryana, India
*Corresponding author, E-mail: jaivir.bmu@gmail.com

ARTICLE HISTORY
Received: 4 Nov. 2022
Revised: 16 Feb. 2023
Accepted: 18 Feb. 2023
Published online: 20 Feb. 2023

KEYWORDS
Stimulated Raman scattering; semiconductor plasmas; hot carriers; narrow band gap semiconductors.

ABSTRACT
Using the hydrodynamic model of semiconductor plasmas, a detailed analytical investigation is made to study both the steady-state and transient Raman gain in a weakly polar narrow band-gap magnetized one-component semiconductor, viz. n-InSb under off-resonant laser irradiation. Using the fact that origin of stimulated Raman scattering (SRS) lies in the third-order (Raman) susceptibility ($\chi_R^{(3)}$) of the medium, we obtained an expression of the threshold pump electric field (E_{th}), the resulting gain coefficients (steady-state as well as transient $g_{R\,TR}$) and optimum pulse duration ($\tau_{_n}$) for the onset of SRS. The application of a strong magnetic field not only lowers E_{th} but also enhances $g_{R.TR}$. The carrier heating by the intense pump modifies the electron collision frequency and hence the nonlinearity of the medium which in turn enhances $g_{R\,TR}$ significantly. The enhanced g_{TR} can be greatly used in the compression of scattered pulses. The results of the present investigation leads to the better understanding of SRS process in solid and gaseous plasmas and also help considerably in filling the existing gap between theory and experiments.

1. Introduction

Nonlinear optics (NLO) is one of the most important fields of modern physics and technology that encompasses the subject of laser-matter interaction [1]. The subject area covered by NLO can be divided into two broad categories: (i) steady-state NLO effects, and (ii) coherent transient optical effects. A large number of NLO effects, such as parametric interactions, self focusing/defocusing, stimulated scatterings, optical phase conjugation, optical bi-stability and their applications to frequency converters and amplifiers and optical signal processing etc., occur as a consequence of either cw laser operation or with lasers having pulse durations much longer than the dephasing or recombination times of the medium. Such nonlinear optical phenomena can be broadly defined as the steady-state NLO effects. The origin of these phenomena in the crystal medium lies largely in anharmonic potentials, free carrier states and photo-generated carriers. On the other hand, the coherent transient optical effects like optical nutation, free induction decay, photon echo and self induced transparency arise when the pulse duration of incident electromagnetic field is much smaller than the dephasing or recombination time of the resonant excited state, the medium can keep in memory the light induced coherence for some time even after switching off the excitation pulse.

Out of several steady-state NLO effects, stimulated scattering of laser radiation continues to be one of the most active areas of research, on one hand, it provides fundamental and microscopic information of the laser matter interaction, and on the other hand it has many applications in the area of modern optics [1, 2]. When an intense coherent light beam propagates in a medium, it may excite the natural mode of vibrations of the medium, i.e., the electron-plasma and ion waves. When one of the excited modes is of high frequency, it gives rise to stimulated Raman scattering (SRS) [3-6]. SRS provides a unique tool for the investigations of possible details of vibrational energetic, life times and dephasing processes. It has been used to extend the tunable range of coherent optical source over a broad spectrum of the infrared regime [7, 8]. Anti-Stokes radiation from SRS with dye lasers can be used to generate tunable ultraviolet sources [9]. Four-wave interactions arising out of third-order polarizability is recently gathering momentum and can also certain conditions give rise to nonlinear devices similar to those based on three wave processes. An important application of such type of interactions in modern optics is to generate Optical Phase Conjugation (OPC) in an active medium [10]. It is well established fact that both coherent and anti-Stokes Raman spectroscopy (CARS) and Raman induced Kerr effect spectroscopy (RIKES) involves the nonlinear four-wave-mixing optical processes.

Various aspects of Raman scattering and its consequent instabilities have been investigated in gaseous plasmas [11-13]. But the practical utilization of semiconductors in drew the attention of many solid-state physicists to examine the role of semiconductors in the areas such as spectroscopy, lasers, device fabrication etc. Moreover, in the search for optical memories and switching elements, one found that the optical properties of these materials change strongly when electrons are excited optically. The electrical properties of semiconductors lie in between those of metals with nearly free electrons and insulators with tightly bound electrons. This

intermediate situation makes semiconductors attractive as nonlinear devices in electronics as well optics because their properties can be influenced easily by fields, compositions and micro-structuring. Hence, the supremacy of semiconductors as active media in laser communication, modern optoelectronic devices, optical computing [14,15] and all optical signal processing [16] is unquestionable and hence the understanding of the mechanisms of transient effects in these crystals appears to be of fundamental significance.

In the recent past, a significant amount of research work on SRS and its consequent instabilities in magnetoactive doped semiconductors have been reported by several groups [17-20]; the theoretical predictions and experimental measurements are far apart. Several experiments, with short laser pulses of low intensity, suggest that SRS starts below the theoretically estimated threshold value, whereas some experiments with high-intensity radiation reveal that SRS signal levels saturate at much lower values than their theoretically predicted values. Neogi and Ghosh have analytically investigated SRS [21] and comparison between SRS and stimulated Brillouin scattering (SBS) [22] in a centrosymmetric magnetized semiconductor and obtained significant Raman growth at pump field strength ~10^8 Vm^{-1}. In a semiconductor crystal, the interaction of this intense pump with carriers results in an appreciable increase in the carrier temperature due to their high mobility, low effective mass, long free path and slow rate of energy transfer to the lattice. Moreover, in the previously reported works, origin of SRS in polar semiconductors has been taken into finiteness of differential polarizability only. However, in these semiconductors, the coupling between pump wave and optical phonon also depends on Szigeti effective charge which cannot be neglected in the infrared regime [23, 24]. Therefore, the inclusion of Szigeti effective charge in theoretical studies of SRS seems to be important from both the fundamental and applied point of view.

Literature survey reveals that no schematic attempt has so far been made to explore the influence of carrier heating on SRS process, where the origin of this process is taken to be in the finiteness of Szigeti effective charge and differential polarizability in narrow band-gap magnetized semiconductors. In the present paper, by using a hydrodynamic model of semiconductor plasma, we intend to study the influence of the pump-induced carrier heating on the steady-state and transient gain coefficients of the Raman mode.

The stimulus for the present study stems from the fact that the carrier heating by the pump can remarkably modify the nonlinearity of the medium and hence the related phenomena. In the wake of high power lasers, such an investigation becomes even more important because it may lead to better understanding of the scattering mechanisms in solid and gaseous plasmas and thus may prove to be a step forward towards filling the gap between theory and experimental observations.

The physical origin of the process lies in the non-vanishing, nonlinear polarization due to the coupling of the molecular vibrations having a frequency equal to that of the transverse optical phonon frequency ω_t with the pump frequency ω_0, as well as the electron plasma frequency ω_p in the presence of a static magnetic field such that $\omega_t < \omega_p < \omega_0$ and $\omega_c (< \omega_0) \gg \omega_\tau [= 0.5(\omega_t^2 + \omega_p^2)^2]$.

2. Theoretical formulations

This section deals with the theoretical formulation of complex effective third-order (Raman) susceptibility $\chi_R^{(3)}$, and there from the steady-state and transient Raman gain coefficients $g_{R,TR}$ for the Stoke's component of the scattered electromagnetic wave in a Raman active medium. We consider the propagation of a hybrid pump wave

$$\vec{E}_0 = (E_{0x}\hat{i} + E_{0y}\hat{j})\exp[i(k_0 x - \omega_0 t)] \quad (1)$$

in a homogeneous semiconductor plasma having an external magnetostatic field $\vec{B}_s = B_{0x}\hat{i} + B_{0z}\hat{k}$ in a direction making an angle θ with the x-axis in the x-z plane, as shown in Figure 1.

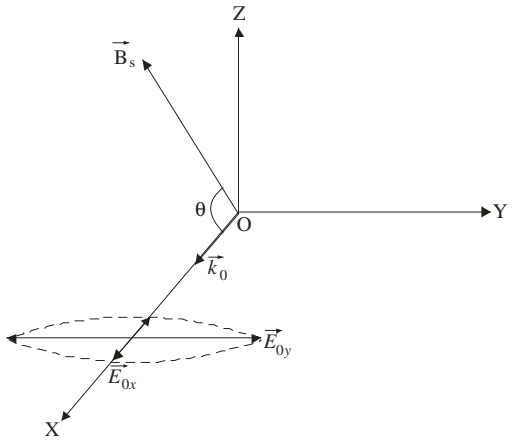

Figure 1: Geometry of SRS in magnetic field.

The authors have chosen this particular field geometry because most of the reported cases correspond to the propagation of a pump wave exactly parallel to the applied magnetic field. Such an exact parallel propagation may not be experimentally feasible. Moreover, the electric field of the pump considered is either perpendicular or parallel to the propagation directions. This, again, is not the case in realistic situations [25]. For a finite solid state plasma, $\vec{E}_0$ must have components that are both parallel and perpendicular to the propagation direction. Thus the most realistic case (that the authors have considered here) is to consider a hybrid mode propagating obliquely to the external magnetic field.

In a Raman active medium the scattering of high frequency pump wave is enhanced due to excitation of a normal vibrational (optical phonon) mode. We consider that the Raman medium consists of N harmonic oscillators per unit volume; each oscillator being characterized by its position x, molecular weight M and normal vibrational coordinates $u(x,t)$.

The equation of motion for a single oscillator (optical phonon) is given by [26]

$$\frac{\partial^2 u(x,t)}{\partial t^2} + \Gamma \frac{\partial u(x,t)}{\partial t} + \omega_t^2 u(x,t) = \frac{F(x,t)}{M} \quad (2)$$

where, Γ is the damping constant equal to the phenomenological phonon-collision frequency ($\sim 10^{-2}\omega_t$) [27]; ω_t being the un-damped molecular vibrational frequency

and is taken to be equal to the transverse optical phonon frequency. $F(x,t)$ is deriving force/ volume experienced by the medium can be put forward as: $F = F^{(1)} + F^{(2)}$, where $F^{(1)}\left(= q_s E\right)$ and $F^{(2)}\left(= 0.5\varepsilon(\partial\alpha/\partial u)_0 \bar{E}^2(x,t)\right)$ describes the forces arising due to Szigeti effective charge q_s and differential polarizability $(\partial\alpha/\partial u)_0$, respectively. The bar over E indicates the averaging over a few optical periods, as the molecules cannot respond to optical frequencies. $\varepsilon = \varepsilon_0\varepsilon_\infty$; ε_0 and ε_∞ are the absolute and high frequencies permittivities, respectively.

The basic equations considered in the present analysis are:

$$\frac{\partial \vec{v}_0}{\partial t} + \nu\vec{v}_0 = \frac{e}{m}[\vec{E}_0 + (\vec{v}_0 \times \vec{B}_s)] = \frac{e}{m}\vec{E}_e \tag{3}$$

$$\frac{\partial \vec{v}_1}{\partial t} + \nu\vec{v}_1 + \left(\vec{v}_0 . \frac{\partial}{\partial x}\right)\vec{v}_1 = \frac{e}{m}[\vec{E}_1 + \vec{v}_1 \times \vec{B}_1] \tag{4}$$

$$\frac{\partial n_1}{\partial t} + n_e\frac{\partial v_1}{\partial x} + n_1\frac{\partial v_0}{\partial x} + v_0\frac{\partial n_1}{\partial x} = 0 \tag{5}$$

$$\vec{P}_{mv} = \varepsilon N(\partial\alpha/\partial u)_0 u^* \vec{E}_e \tag{6}$$

$$\frac{\partial E_{1x}}{\partial x} = -\frac{n_1 e}{\varepsilon} - \frac{1}{\varepsilon}\frac{\partial P}{\partial x} \tag{7}$$

Eqs. (3) and (4) represent the rate equations for the pump and signal beams under the influence of a magnetostatic field, respectively. $\vec{B}_s$, $\vec{B}_1$ and $\vec{v}_0$, $\vec{v}_1$ are, respectively, the equilibrium and perturbed magnetic fields and oscillatory fluid velocities of the electrons of effective mass *m* and charge *e*. ν is the electron collision frequency. In Eq. (3), $\vec{E}_e$ represents the effective electric field which includes the Lorentz force ($\vec{v}_0 \times \vec{B}_s$) due to external magnetic field and is given by $\vec{E}_e = \vec{E}_0 + (\vec{v}_0 \times \vec{B}_s)$. The electron continuity equation is given by Eq. (5) in which n_e and n_1 are the equilibrium and perturbed current densities, respectively. $\vec{P}_{mv}$ given by Eq. (6) is the nonlinear polarization due to natural mode of vibrations driven by the electric field. Space charge field $\vec{E}_1$ is determined by Poisson's equation (Eq. (7)), in which the second term is due to differential polarizability of the medium. The molecular vibrations at frequency ω causes a modulation of the dielectric constant of the medium leading to an exchange of energy between the electromagnetic fields separated in frequency by multiples of ω (i.e., ($\omega_0 \pm p\omega$), where p = 1, 2, 3, …). The modes at frequencies $\omega_0 + p\omega$ are known as anti-Stoke's modes; while those at $\omega_0 - p\omega$ are Stoke's modes. As we are interested only in first-order Stoke's component of scattered electromagnetic mode, the energy and momentum phase matching conditions to be satisfied are: $\hbar\omega_s = \hbar\omega_0 - \hbar\omega$, $\hbar\vec{k}_s = \hbar\vec{k}_0 - \hbar\vec{k}$. Here ($\omega_s, \vec{k}_s$) represents the Stoke's modes.

2.1 Induced current density

The high frequency pump field gives rise to a carrier density perturbation, which in turn derives an electron-plasma wave and induces current density in the Raman active medium. Now following the standard approach adopted by Sen and Sen. [17] for the theoretical development the perturbed electron density (n_t) of the Raman active medium due to molecular vibrations can be deduced from equations (2) – (7) as:

$$n_t = \frac{i\varepsilon k}{e}\left[\frac{(\omega_t^2 - \omega^2 + i\omega\Gamma) - (\varepsilon N/2M)Q_\alpha}{(\varepsilon/2M)(\partial\alpha/\partial u)_0 (E_e)_x^*}\right]u^*. \tag{8}$$

where $Q_\alpha = \left\{2(q_s/\varepsilon)(\partial\alpha/\partial u)_0\right\} - (\partial\alpha/\partial u)_0^2\left|(E_e)_x\right|^2$.

The density perturbation associated with the molecular vibrations at frequency ω beats with the pump at frequency ω_0 and produces fast components of density perturbations. The Stokes mode of this component at frequency $\omega_s = \omega_0 - \omega$ is obtained as:

$$n_s = \frac{ie(k_0 - k)(E_e)_x}{m(\delta_1^2 - i\nu\omega_s)} n_t^*, \tag{9}$$

where $\delta_1^2 = \bar{\omega}_r^2 - \omega_s^2$ and suffixes *t* and *s* denote the components of the perturbed carrier concentration associated with normal vibrations in the medium and the first-order Stoke's mode respectively. In Eq. (9)

$$\bar{\omega}_r^2 = \omega_r^2\left[\frac{\omega_{cx}^2 + \nu^2}{\omega_c^2 + \nu^2}\right], \text{ in which } \omega_r^2 = \frac{\omega_p^2\omega_l^2}{\omega_t^2},$$

$$\omega_{cx,z}\left(= \frac{eB_{sx,z}}{m}\right),\ \omega_p = \left(\frac{n_e e^2}{m\varepsilon_0\varepsilon_L}\right)^{1/2}, \text{ and } \frac{\omega_l}{\omega_t} = \left(\frac{\varepsilon_L}{\varepsilon_\infty}\right)^{1/2}.$$

ω_l is the longitudinal optical phonon frequency and is given by $\omega_l = k_B\theta_D/\hbar$, where k_B and θ_D are Boltzmann constant and Debye temperature of the lattice, respectively. ε_L is the lattice dielectric constant.

The components of oscillatory electron fluid velocity in the presence of pump and the magnetostatic fields are obtained from Eq. (3) as:

$$v_{0x} = \frac{\bar{E}}{\nu - i\omega_0}, \tag{10a}$$

$$v_{0y} = \frac{(e/m)[\omega_{cz}E_{0x} + (\nu - i\omega_0)E_{0x}]}{[\omega_{cz}^2 + (\nu - i\omega_0)^2]}. \tag{10b}$$

Now the resonant Stoke's component of the current density due to finite nonlinear polarization of the medium has been deduced by neglecting the transient dipole moment, which can be represented as:

$$\vec{J}_{cd}(\omega_s) = n_e e\vec{v}_{1x} + n_s^* e\vec{v}_{0x}, \tag{11}$$

which yields

$$\vec{J}_{cd}(\omega_s) = \frac{\varepsilon\omega_p^2 E_{1x}}{(\nu - i\omega_s)} + \frac{\varepsilon k(k_0 - k)\left|\bar{E}_0\right|^2 E_{1x}}{(\delta_1^2 + i\nu\omega_s)(\nu - i\omega_s)} \times \left[1 - \frac{(\varepsilon N/2M)Q_\alpha}{(\delta_2^2 + i\Gamma\omega)}\right], \tag{12}$$

where $\delta_2^2 = \bar{\omega}_r^2 - \omega^2$.

The first term of Eq. (12) represents the linear component of the induced current density while the second-term represents the nonlinear coupling amongst the three interacting waves via the nonlinear current density.

2.2 Threshold pump amplitude and optical susceptibilities

To begin with, let us treat the induced polarization $\vec{P}_{cd}(\omega_s)$ as the time integral of the current density $\vec{J}_{cd}(\omega_s)$, then one gets

$$\vec{P}_{cd}(\omega_s) = \int \vec{J}_{cd}(\omega_s)dt = \frac{-\vec{J}_{cd}(\omega_s)}{i\omega_s}. \tag{13}$$

Using the approach of Singh et.al. [28], we obtain the nonlinear induced polarization using perturbed current density

$$\vec{P}_{cd}(\omega_s) = \frac{e^2\varepsilon_\infty k(k_0-k)\left|\vec{E}_0\right|^2\vec{E}_{1x}}{m^2\omega_0\omega_s(\delta_1^2+i\nu\omega_s)}\times\left[1-\frac{(\varepsilon N/2M)Q_\alpha}{(\delta_2^2+i\Gamma\omega)}\right]. \tag{14}$$

From the above relation we can determine the nature of the threshold for the onset of SRS process by setting $P_{cd}(\omega_s)=0$. This condition yields,

$$E_{th} = \frac{m}{ek}\frac{\delta_1\delta_2(\omega_0^2-\omega_c^2)}{[(\omega_0^2-\omega_{cx}^2)+\nu\omega_{cz}]}. \tag{15}$$

This equation reveals that E_{th} is strongly influenced by the material parameters (n_e, v), the magnetic field (ω_c) and the geometry θ of the magnetic field.

In addition to the polarization $\vec{P}_{cd}(\omega_s)$, the system should also possess a polarization created by the interaction of the pump wave with the molecular vibrations generated within the medium, obtained from equations (2) and (6) as:

$$\vec{P}_{mv}(\omega_s) = \frac{\varepsilon\omega_0^2(\varepsilon N/2M)(\partial\alpha/\partial u)_0^2\left|E_0\right|^2\vec{E}_{1x}}{(\delta_2^2+i\Gamma\omega)}. \tag{16}$$

Thus, the total polarization induced at the Stoke's component for a pump amplitude well above the threshold is given by

$$\vec{P}(\omega_s) = \vec{P}_{mv}(\omega_s)+\vec{P}_{cd}(\omega_s) = \left[\frac{\varepsilon\omega_0^2(\varepsilon N/2M)(\partial\alpha/\partial u)_0^2}{(\delta_2^2+i\Gamma\omega)}+\frac{e^2\varepsilon_\infty k(k_0-k)}{m^2\omega_0\omega_s(\delta_1^2+i\nu\omega_s)}\times\left\{1-\frac{(\varepsilon N/2M)Q_\alpha}{(\delta_2^2+i\Gamma\omega)}\right\}\right]\left|E_0\right|^2\vec{E}_{1x}. \tag{17}$$

Now it is well known that, the origin of SRS process lies in that component of $\vec{P}(\omega_l)$ which depends on $\left|\vec{E}_0\right|^2\vec{E}_{1x}$. The corresponding effective third-order susceptibility (also known as Raman susceptibility $\chi_R^{(3)}$) is given by:

$$\chi_R^{(3)} = \chi_{mv}^{(3)}+\chi_{cd}^{(3)} = \frac{\varepsilon\omega_0^2(\varepsilon N/2M)(\partial\alpha/\partial u)_0^2}{(\delta_2^2+i\Gamma\omega)}+\frac{e^2\varepsilon_\infty k(k_0-k)}{m^2\omega_0\omega_s(\delta_1^2+i\nu\omega_s)}\times\left\{1-\frac{(\varepsilon N/2M)Q_\alpha}{(\delta_2^2+i\Gamma\omega)}\right\} \tag{18}$$

Here $k=(k_0^2+k_s^2-2k_0k_s\cos\phi)^{1/2}$, where ϕ is the scattering angle between $\vec{k}_s$ and $\vec{k}_0$. It is evident from Eq. (18) that $\chi_R^{(3)}$ is strongly dependent on q_s and $(\partial\alpha/\partial u)_0$.

2.3 Carrier heating and modified nonlinearity

To incite SRS, the fundamental requirement is to apply a pump field above the threshold value. When this high-intensity pump traverses a high mobility semiconductor, the carriers acquire momentum and energy from the pump and as a result they (here electrons) acquire a temperature (T_e) somewhat higher than that of the lattice (T_0). This field-dependent rise in the electron temperature, in turn, modifies the electron collision frequency (ECF) through the relation [29]:

$$\nu = \nu_0\left(\frac{T_e}{T_0}\right)^{1/2} \tag{19}$$

where ν_0 is the ECF in the absence of the pump, i.e. at $T_e = T_0$. The temperature ratio (T_e/T_0) can be readily obtained from energy balance equation in the following manner.

The power absorbed per electron from the pump may be obtained as [30]:

$$\frac{e}{2}\mathrm{Re}\left[\vec{v}_{0x}.\vec{E}_e^*\right] = \frac{e^2\nu}{2m}\frac{(\omega_0^2+\omega_c^2)}{[(\omega_0^2+\omega_c^2)+4\nu^2\omega_0^2]}\left|\vec{E}_0\right|^2 \tag{20}$$

where the asterisk denotes the complex conjugate while Re stands for the real part of the quantity concerned. The *x*-component of $\vec{v}_0$ used in the above relation may be evaluated from Eq. (10a).

Following Conwell [31], the power dissipation per electron in collisions with the POP may be expressed as:

$$\left(\frac{\partial\in}{\partial t}\right)_{diss} = \left(\frac{2k_B\theta_D}{m\pi}\right)^{1/2}eE_{PO}(x_e)^{1/2}K_0\left(\frac{x_e}{2}\right).\exp\left(\frac{x_e}{2}\right).\frac{\exp(x_0-x_e)-1}{\exp(x_0)-1} \tag{21}$$

where $x_{0,e}=\dfrac{\hbar\omega_l}{k_BT_{0,e}}$, $\vec{E}_{PO}=\dfrac{me\hbar\omega_l}{\hbar^2}\left(\dfrac{1}{\varepsilon_\infty}-\dfrac{1}{\varepsilon}\right)$,

$\hbar\omega_l$ is the energy of the POP and is given by $\hbar\omega_l = k_B\theta_D$ and θ_D is the Debye temperature of the crystal; ε and ε_∞ are the static and high frequency dielectric permittivities of the medium, respectively. $K_0(x_e/2)$ is the zeroth-order Bessel function of the first kind. In steady-state, the power absorption per electron from the pump is just equal to the power lost in

collisions with POP. For moderate heating of the carriers, Eq. (19) and (20) yield

$$\frac{T_e}{T_0} = 1 + \alpha \left| \vec{E}_0 \right|^2 . \tag{22}$$

where $\alpha = \dfrac{e^2 v_0 \tau}{2 m \omega_0^2}$ (23a)

in which

$$\tau^{-1} = \left(\frac{2 k_B \theta_D}{m \pi} \right)^{1/2} e E_{PO} K_0 \left(\frac{x_0}{2} \right) \frac{x_0^{1/2} \exp(x_0/2)}{\exp(x_0) - 1} . \tag{23b}$$

Thus the modified ECF may be obtained as:

$$\nu = \nu_0 \left(1 + \alpha \left| \vec{E}_0 \right|^2 \right)^{1/2} \approx \nu_0 \left(1 + \frac{1}{2} \alpha \left| \vec{E}_0 \right|^2 \right) \tag{24}$$

By incorporating this modified ECF in Eq. (18), one can study the influence of carrier heating on third-order (Raman) susceptibility.

2.4 Steady-state and transient Raman gain coefficients of Stokes component

The steady state Raman gain coefficient of the Stoke's component in the presence of a pump well above the threshold value is obtained as:

$$g_R(\omega_s) = -\frac{\omega_s}{\eta c_0} \left[\chi_R^{(3)} \right]_i \left| \vec{E}_0 \right|^2 = \frac{\varepsilon_\infty \omega_s \omega_0^2 E_0^2}{2 m^2 \eta c_0 (\omega_0^2 - \omega_c^2)} \frac{\left[\omega m^2 (\varepsilon N / 2M) Q_\alpha (\omega_0^2 - \omega_c^2)(\delta_2^4 + \nu^2 \omega_s^2) - e^2 k^2 \nu \omega_0 (\delta_1^4 + \Gamma^2 \omega^2) \right]}{\left[(\delta_1^2 \delta_2^2 - \nu \Gamma \omega \omega_s)^2 + (\nu \omega_s \delta_1^2 + \Gamma \omega \delta_2^2)^2 \right]} \tag{25}$$

Eq. (25) reveals that $g_R(\omega_s)$ increases quadratically with increasing pump electric field. Practically, however, the pump field strength cannot be increased arbitrary because it may damage the sample. Mayer et.al. [32] pointed out that when a semiconductor is irradiated with an intense laser light with long pulse duration a frequent consequent is the product of heat.

For example, a typical pump field strength $E_0 = 0.86 \times 10^7\ \mathrm{Vm^{-1}}$ (corresponding intensity $4.2 \times 10^{11}\ \mathrm{Wm^{-2}}$) of Q-switched 170 ns pulse 10.6 μm CO_2 laser damages InSb at 300 K [33].

It is worth pointing out that for $E_0 = 7 \times 10^7\ \mathrm{Vm^{-1}}$), the first term of parameter Q_α in Eq. (25) dominates over second and Raman gain is due to the finiteness of q_s and $(\partial \alpha / \partial u)_0$. However for $E_0 > 7 \times 10^7\ \mathrm{Vm^{-1}}$, the contribution of effective charge is wiped off ($q_s = 0$) and Raman gain spectrum becomes dependent only on differential polarizability.

This case (with $q_s = 0$) sports the theory developed by Neogi et.al. [21]. Thus the present formulation replaces the prevailing concept of using high power pump field strength to get efficiently large steady-state Raman gain coefficient in narrow band gap magnetoactive semiconductors.

We can find that the above formulations are very much handicapped not only in predicting the optimum pulse durations for which the Raman gain can be observed but also in predicting the threshold pump intensity for the onset of Raman instability. This reveals that SRS should be treated by incorporating the transient effects. In general, the transient Raman gain coefficient (g_{TR}) is related to the steady-state gain coefficient through [34]

$$g_{TR} = [2 g_R x \Gamma_R \tau_p]^{1/2} - \Gamma_R \tau_p \tag{26}$$

where Γ_R is the optical phonon lifetime, x is the interaction length, and τ_p is the pulse duration. For backward SRS at very short pump pulse duration ($\tau_p \le 10^{-10}\ \mathrm{s}$), the interaction length should be replaced by $c_L \tau_p / 2$, where $c_L (= c_0 \sqrt{\varepsilon_L})$ is the velocity of light in the crystal lattice.

Consequently, by making $g_{TR} = 0$ in Eq. (26), we obtained the threshold pump intensity for the onset of transient SRS as:

$$I_{th} = \frac{\Gamma_R}{2 G_R c_L} , \tag{27}$$

where $G_R = g_R / I_p$ is the steady state Raman gain coefficient per unit pump intensity and $I_p = (1/2) \eta \varepsilon_0 c \left| \vec{E}_0 \right|^2$.

Using $\Gamma_R = 3.7 \times 10^{11}\ \mathrm{s^{-1}}$ and $g_R = 50\ \mathrm{m^{-1}}$ at $I_p = 2.88 \times 10^9\ \mathrm{Wm^{-2}}$ for a weakly polar semiconductor-plasma and Eq. (27), we obtain the threshold value of pump intensity for the onset of Raman instability as $1.5 \times 10^{11}\ \mathrm{Wm^{-2}}$.

However, for comparatively long pulse duration ($\tau_p \ge 10^{-9}\ \mathrm{s}$), the cell length can be taken equal to x, and under such circumstances, we finds

$$g_{TR} = (\Gamma_R \tau_p)^{1/2} [-(\Gamma_R \tau_p)^{1/2} + (g_R x)^{1/2}] . \tag{28}$$

The above expression gives an idea about the optimum pulse duration $\tau_{p,opt}$, above which no transient gain could be achieved by making $g_{TB} = 0$, which yields:

$$\tau_{p,opt} \approx \frac{g_R}{\Gamma_R} . \tag{29}$$

The values of $\tau_{p,opt}$ suggest that optimum pulse duration can be increased by increasing the pump intensity. Eq. (29) explains the washing out of Raman gain at large pulse durations. A calculation for weakly polar semiconductor-plasma using the values given earlier and $x = 10^{-4}\ \mathrm{m}$, gives $\tau_{p,opt} = (5.6 \times 10^{-20} I_p)\ \mathrm{s}$.

3. Results and discussion

In order to establish the validity of present model and to study SRS process, we have chosen a weakly-polar narrow band-gap semiconductor crystal (n-InSb) at 77 K as the medium, which is assumed to be irradiated by a 10.6 μm CO_2

laser of frequency $\omega_0 = 1.78\times10^{14}\ s^{-1}$. The physical parameters are taken from Ref. [17, 18].

Using the material parameters given above, the nature of dependence of the threshold pump amplitude E_{th} on magnetic field strength (in terms of ω_c/ω_0) with magnetic field inclination θ as a parameter is investigated in the InSb crystal and is plotted in Figure 2.

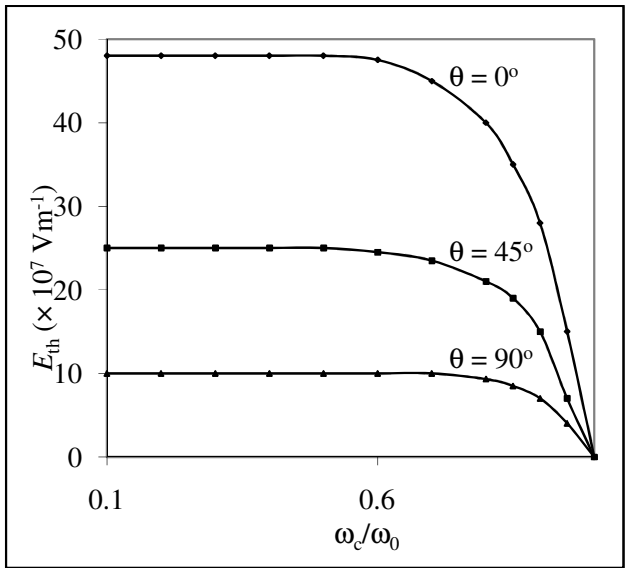

Figure 2: Dependence of threshold pump amplitude E_{th} on magnetic field strength (in terms of ω_c/ω_0) for $\theta = 0^o$, $\theta = 45^o$ and $\theta = 90^o$. Here $n_e = 10^{24}\,m^{-3}$, $\phi = \pi/6$.

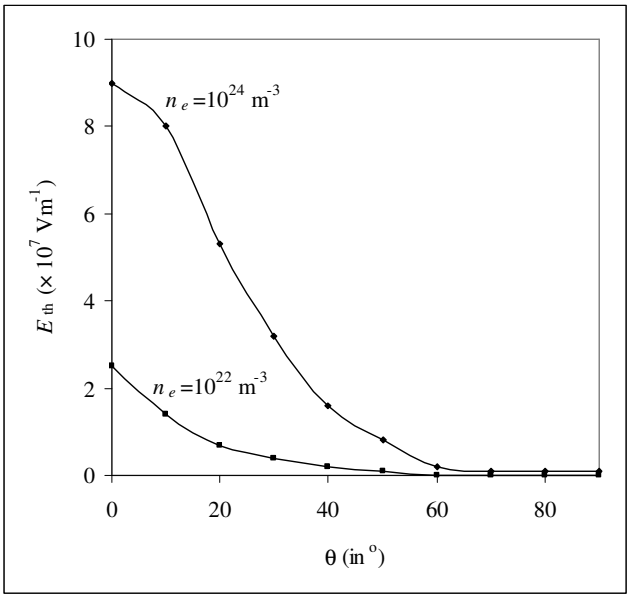

Figure 3: Dependence of threshold pump amplitude E_{th} on magnetic field inclination θ for $n_e = 10^{22}$ and $10^{24}\,m^{-3}$. Here $\omega_c = 0.9\omega_0$, $\phi = \pi/6$.

In all the cases, E_{th} starts with a relatively high value, at $\omega_c = 0.1\omega_0$, remains constant up to $\omega_c = 0.7\omega_0$, and thereafter decreases sharply with increasing ω_c. For strong magnetic field, E_{th} becomes independent of θ and the curves coincide.

Figure 3 illustrates the dependence of E_{th} on the magnetic field inclination θ. In the presence of a longitudinal field, a heavily doped medium requires an order larger threshold field in comparison with that of moderately doped medium. However, as θ increases E_{th} decreases and the gap between the E_{th} curves narrows down. For $\theta \to 90^o$; the two curves approach each other indicates that magnetic field makes E_{th} independent of carrier concentration.

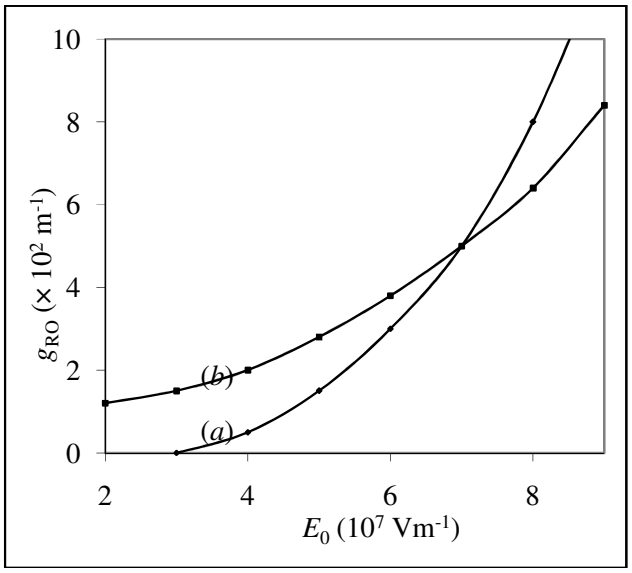

Figure 4: (a) Variation of steady-state Raman gain coefficient g_{RO} (in the absence of carrier heating) as a function of pump field strength E_0 for $q_s = 0$ (curve (*a*)) and $q_s \neq 0$ (curve (b)).

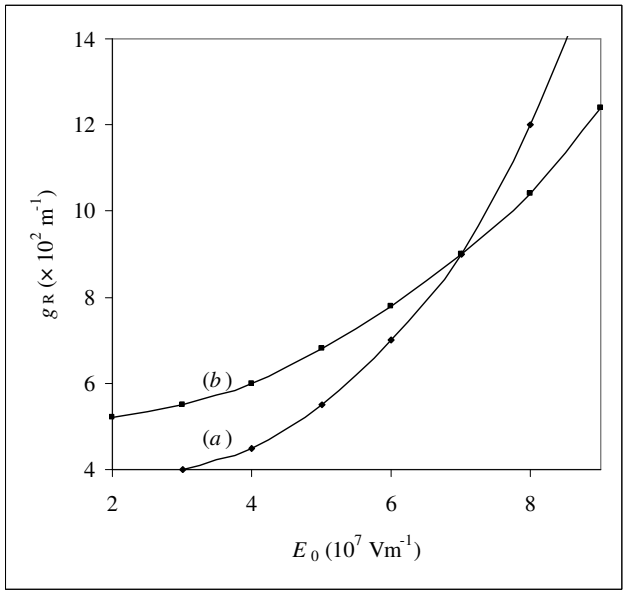

Figure 4: (b) Variation of steady-state Raman gain coefficient g_R (in the presence of carrier heating) as a function of pump field strength E_0 for $q_s = 0$ (curve (*a*)) and $q_s \neq 0$ (curve (b)). Here $n_e = 10^{24}\,m^{-3}$, $\omega_c = 0.9\omega_0$, $\phi = \pi/6$, $\theta = \pi/4$.

Being one of the principal objectives of the present analysis, the nature of dependence of steady-state Raman gain coefficients g_{RO} (in the absence of carrier heating) and g_R (in the presence of carrier heating) as a function of pump field strength E_0 for $q_s = 0$ (curve (*a*)) and $q_s \neq 0$ (curve (b)) has been analyzed in Figs. 4(a) and 4(b) respectively. In both cases

Raman gain increases with input pump field strength for $q_s = 0$ and $q_s \neq 0$ [Eq. 25]. It is interesting to note that for $E_0 < E_c \left(= 7\times10^7\ \mathrm{V m^{-1}}\right)$, the contribution of Szigeti effective charge q_s is more as compared to differential polarizability $(\partial\alpha/\partial u)_0$. However, for $E_0 > E_c$, Raman gain is due to differential polarizability. This is due to the fact that at pump field strength $E_0 > E_c$, the second term in Q_α of Eq. (25) dominates over the first and the contribution of q_s is nearly wiped off. At particular value of pump field strength $E_0 = E_c$, q_s and $(\partial\alpha/\partial u)_0$ contributes equally to steady-state Raman coefficients. Thus the incorporation of Szigeti effective charge in the analysis replaces the prevailing concept of using high pump field strengths to obtain significant steady-state Raman gain.

While comparing the results of Figure 4(a) and 4(b), the most striking feature is that the steady-state Raman gain coefficient g_R (in the presence of carrier heating) is found to be 4.33 times g_{RO} (in the absence of carrier heating). This enhancement of steady-state Raman gain coefficient may be attributed to increase in ECF [Eq. (24)] due to carrier heating. The increase in ECF apparently results in an increase in energy transfer of the pump and Stoke's mode and subsequently enhances steady-state Raman gain.

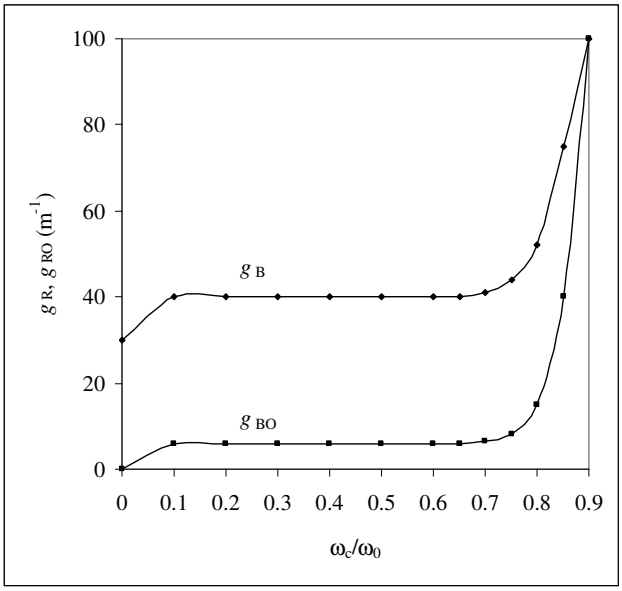

Figure 5: Variation of steady state Raman gain coefficients g_R and g_{RO} as a function of magnetic field strength (in terms of ω_c/ω_0). Here $E_0 = 7\times10^7\ \mathrm{V m^{-1}}$, $n_e = 10^{24}\ \mathrm{m^{-3}}$, $\phi = \pi/6$, $\theta = \pi/4$.

Figure 5 depicts the variation of steady state Raman gain coefficients g_R and g_{RO} as a function of magnetic field strength. It is a unique feature displaced in this figure that both the gain coefficients are found fairly independent of lower magnetic field. But as ω_c approaches ω_0, the gain coefficients increase rapidly. Thus a higher magnitude of steady-state Raman gain coefficients is obtained at $\omega_c \sim \omega_0$ which is independent of magnetic field. Hence, the stimulated laser may be tuned by operating the magnetic field (cyclotron frequency) around the pump frequency; a similar result reported in the case of steady-state gain coefficient by Neogi et.al. [22].

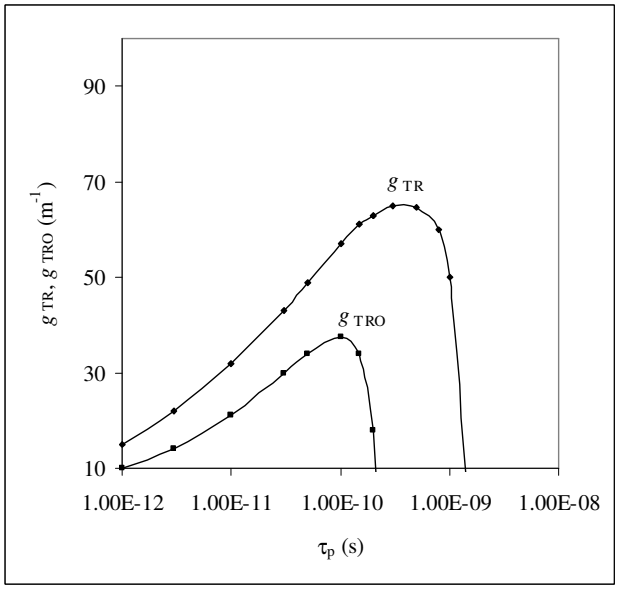

Figure 6: Variation of transient Raman gain coefficients g_{TR} and g_{TRO} as a function of pump pulse duration τ_p. Here $I_p = 2\times10^{13}\ \mathrm{W m^{-2}}$, $n_e = 10^{24}\ \mathrm{m^{-3}}$, $\omega_c = 0.9\omega_0$, $\phi = \pi/6$, $\theta = \pi$.

Figure 6 depicts the influence of pump pulse duration τ_p on the transient Raman gain of Stoke's mode. Here g_{TR} and g_{TRO} denote the transient Raman gain coefficients with and without incorporating carrier heating by the pump, respectively. To draw this behaviour, we have considered pulse durations in the range $10^{-12} \le \tau_p \le 10^{-8}$ s and pump field intensity $I_p = 4.8\times10^{12}\ \mathrm{W m^{-2}}$. The interaction length is the cell length x. The gain coefficients increases with pulse duration and at a certain value of τ_p, both g_{TR} and g_{TRO} attains a maximum value which remains constant for a certain range of τ_p. Such regions can be regarded as quasi-steady states or quasi-saturation regimes. The presence of carrier heating enhances the transient Raman gain coefficient shifts the gain saturation regime towards higher value of τ_p. The enhancement in g_{TR} may be attributed to increase in ECF which results in an increase in energy transfer of the pump and Stokes mode and subsequently enhances g_{TR}. If τ_p is chosen beyond the quasi-saturation regime, the transient gain coefficients diminishes very rapidly. This behaviour is very much similar to experimental observations with CS_2 [35] of the saturation of Raman conversion efficiency which is proportional to the exponential of the gain factor, to a very low value at longer pulse duration. Thus incorporation of carrier heating in the analysis not only makes our model realistic and the analysis more reliable but may also considerably minimize discrepancies between the experimental observations and theoretical predictions.

4. Conclusions

The present work deals with the analytical investigations of steady-state and transient Raman gain in weakly polar narrow band-gap magnetized semiconductors duly shined by a pulsed 10.6 μm CO_2 laser. The role of carrier heating by the pump has been examined at length. The carrier heating by the pump appreciably enhances the ECF and hence transfers energy from the pump to the scattered light. As a result, the

steady state as well as transient Raman gain coefficients are considerably enhanced. Thus, incorporation of carrier heating by the pump may help in reducing discrepancies between theory and experimental measurements. This may be an important step towards the appropriate interpretation of experimental measurements in solid and gaseous plasmas. The presence of external strong magnetic field in the transverse direction significantly reduces the threshold pump field for the onset of SRS and enhances the steady-state and transient Raman gain coefficients in weakly polar narrow band-gap semiconductors. For pump field strength $E_0 < E_c$, the contribution of Szigeti effective charge is more as compared to differential polarizability. However, for $E_0 > E_c$, Raman gain is due to differential polarizability. At particular value of pump field strength $E_0 = E_c$, Szigeti effective charge and differential polarizability contributes equally to steady-state Raman coefficients. The incorporation of Szigeti effective charge in the analysis replaces the prevailing concept of using high pump field strengths to obtain significant steady-state Raman gain. The presence of carrier heating enhances the transient Raman gain coefficient and shifts the gain saturation regime towards higher value of pump pulse duration. Semiconductor plasmas duplicate gaseous plasmas as far as phenomena of waves and instabilities are concerned. From this viewpoint, semiconductors may be used as a compact and convenient substitute for gaseous plasmas on account of their considerable ease of operation, liberty of manipulating the material parameters over a wide range, and lack of confinement problems. Thus, the present study may also be used to develop a clearer understanding of stimulated scattering mechanisms and their threshold values encountered in laser induced plasmas.

Acknowledgements

The author is very thankful to Dr. Manjeet Singh, Assistant Professor, Department of Physics, Government College, Matanhail, Jhajjar – 124106 (Haryana) India for many useful suggestions to carry out this research work and careful reading of the manuscript.

References

[1] R.L. Sutherlands, *Handbook of Nonlinear Optics*, Marcel Dekker, New York (2003).
[2] S.I. Anisimov, V.A. Khokhlov, *Instabilities in Laser Matter Interaction*, Academic Press, New York (1995).
[3] K.A. Brueckner, S. Jorna, Laser-driven fusion, *Rev. Mods. Phys.* **46** (1974) 325-367.
[4] C.S. Liu, M.N. Rosenbluth, R.B. White, Raman and Brillouin scattering of electromagnetic waves in inhomogeneous plasmas, *Phys. Fluids* **17** (1974) 1211-1219.
[5] J.F. Drake, P.K. Kaw, Y.C. Lee, G. Schmidt, C.S. Liu, M.N. Rosenbluth, Parametric instabilities of electromagnetic waves in plasmas, *Phys. Fluids* **17** (1974) 778-785.
[6] D.W. Forslund, J.M. Kindel, E.L. Lindman, Nonlinear behaviour of stimulated Brillouin and Raman scattering in laser irradiated plasmas, *Phys. Rev. Lett.* **30** (1973) 739-743.
[7] D.C. Hanna, M.A. Yuratich, D. Cottor, *Nonlinear Optics of Free Atoms and Molecules*, Springer, Berlin (1979), ch. 7.
[8] T.R. Loree, R.C. Sze, D.L. Barker, P.B. Scott, New lines in the UV: SRS of excimer laser wavelengths, *IEEE J. Quantum Electron.* **15** (1979) 337-342.
[9] J.E. Rothenberg, J.F. Young, S.E. Harris, High-resolution extreme ultraviolet spectroscopy of potassium using anti-Stoke's radiation, *Opt. Lett.* **6** (1981) 363-365.
[10] B.Y. Zeldovich, N.F. Pilipetsky, V.V. Shkunov, *Principles of Phase Conjugation*, Springer, Berlin (1985), p. 25.
[11] M.S. Sodha, R.P. Sharma, S.C. Kaushik, Interaction of intense laser beams with plasma waves: stimulated Raman scattering, *J. Appl. Phys.* **47** (1976) 3518-3523.
[12] B. Maraghechi, J.E. Willett, Raman backscattering of electromagnetic extraordinary waves in a magnetized inhomogeneous plasma, *J. Plasma Phys.* **20** (1978) 859-865.
[13] B. Maraghechi, J.E. Willett, Raman backscattering of circularly polarized electromagnetic waves propagating along a magnetic field, *J. Plasma Phys.* **21** (1979) 163-172.
[14] C.H. Lee, *Picosecond Optoelectronic Devices*, Academic Press, New York (1984), pp. 1-9, 119-188, 219-284.
[15] H.N. Gibbs, *Optical Bistability: Controlling Light with Light*, Academic, Orlando (1985).
[16] B.S. Wherrett, *Optical Computing*, SUSSP, Edinburg (1989), pp. 1-21.
[17] P.K. Sen, N. Apte, S. Guha, Raman instability in n-type piezoelectric semiconductors, *Phys. Rev. B* **22** (1980) 6340-6346.
[18] P. Sen, P.K. Sen, Theory of stimulated Raman and Brillouin scattering in noncentrosymmetric crystals, *Phys. Rev. B* **31** (1985) 1034-1040.
[19] P. Sen, P.K. Sen, Correlation and competition between stimulated Raman and Brillouin scattering processes, *Phys. Rev. B* **33** (1986) 1427-1435.
[20] S. Ghosh, S. Dixit, Stimulated Raman scattering and Raman instability of an intense helicon wave in longitudinally magnetized n-type piezoelectric semiconducting plasma, *Phys. Stat. Sol. (b)* **131** (1985) 255-265.
[21] A. Neogi, S. Ghosh, Stimulated Raman scattering in a magnetized centrosymmetric semiconductor, *Phys. Rev. B* **44** (1991) 13074-13077.
[22] A. Neogi, S. Ghosh, D.K. Sinha, Stimulated scattering in magnetooactive semiconductors, *Phys. Rev. B* **47** (1993) 16590-16593.
[23] J. Callaway, *Quantum Theory of the Solid State*, Academic Press, New York (1974), p. 16.
[24] K. Seeger, *Semiconductor Physics*, Springer-Verlag, Berlin (1989), p. 183.
[25] M.C. Steele, B. Vural, *Wave interactions in Solid State Plasmas*, McGraw Hill, New York (1969), p. 105.
[26] S.D. Kramer, F.G. Parsons, N. Bloembergen, Interference of third-order light mixing and second harmonic exciton generation in CuCl, *Phys. Rev. B* **9** (1974) 1853-1856.
[27] K. Nishikawa, Parametric excitation of coupled waves 1. General Formulation, *Phys Soc Jpn* **24** (1968) 916-922.
[28] M. Singh, P. Aghamkar, Coherent Brillouin scattering in non-centrosymmetric semiconductors: bound and free charge carriers contribution, *J. Mod. Opt*. **55** (2008) 1251-1265.
[29] A.C. Beer, *Galvanometric Effects in Semiconductors: Solid State Physics*, Academic Press, New York (1963).
[30] M.S. Sodha, A.K. Ghatak, V.K. Tripathi, *Self-Focusing of Laser Beams in Dielectrics, Plasmas and Semiconductors*, Tata McGraw, New Delhi (1974), pp. 55-62.
[31] E.M. Conwell, *High Field Transport in Semiconductors*, Academic Press, New York (1967), pp. 159.
[32] J.M. Mayer, F.J. Bartoli, M.R. Kruer, Optical heating in semiconductors, *Phys. Rev. B* **21** (1980) 1559-1568.
[33] M. Kruer, L. Esterowitz, F. Bartoli, R. Allea, *Laser Induced*

Damage in Optical Materials, A.J. Glass, A.H. Guenther (Ed.), NBS Special Publication No. 509, Washington (1977), p. 473.
[34] C.S. Wang, *Quantum Electronics*, Academic Press, New York (1975), pp. 447-472.
[35] D. Vonder Linde, A. Laubereau, W. Kaiser, Molecular vibrations in liquids: direct measurement of the molecular dephasing time: determination of the shape of picosecond light pulses, *Phys. Rev. Lett*. **26** (1971) 954-957.